MILLIMETER ARRAY
MEMO NO. 43

A comparison of a mosaiced VLA image and a conventional Penticton image

T. J. CORNWELL

National Radio Astronomy Observatory,[a] Socorro, New Mexico 87801

INTRODUCTION

The millimeter array will form images of large objects by "mosaicing", probably using a Maximum Entropy algorithm (Cornwell 1984). As part of the continuing design of the MMA, we plan to investigate the capabilities and limitations of this method. For this, we will use a three-pronged approach: theory (e.g. Cornwell 1987), simulation, and experiment. This memo describes an experiment using both the VLA and the Penticton array to image a large ($\sim$ 2.5 degree) source, Simeis 57, at λ20cm.

THE OBSERVATIONS

Penticton: A standard full synthesis of Simeis 57 was made. The data was calibrated with respect to the Baars scale. The spacings range from 12.8m up to 600m in increments of 4.5m (i.e. half the element diameter). The mean observing frequency was 1420.875MHz, but the band was split into two chunks sufficiently separated in frequency that all Galactic hydrogen was avoided. The appropriate coordinate system for the images produced is the AIPS NCP geometry. Dirty images and beams of size 1024^2 pixels were made using the AIPS task UVMAP. Uniform weighting was used. To avoid super-resolution in the deconvolution, the dirty image was then "pre-convolved" with a circular Gaussian of FWHM 45 arcseconds of unit sum. This resolution is slightly smaller than that of Penticton ($\sim$ 75 by 50 arcseconds), but is comparable to that of the VLA. The primary beam was modeled by a circular Gaussian of FWHM equal to 104 arcminutes. The deconvolution was performed using the AIPS task VTESS. Typically about 12 iterations were required for convergence to a noise level of 900 μJy/beam. After deconvolution, the geometry was converted to the AIPS SIN projection using HGEOM.

VLA: Simeis 57 was observed in a mosaic of pointings spanning the 2.5 degrees of this object. The data was calibrated with respect to the Baars scale. The observing frequency was 1395.000MHz. To minimise the computing required, the pointings were placed only on the brightest parts of the Penticton image, neccessitating 22 pointings in all. These were spread on a rectangular grid, spaced every half-width-to-half-maximum (15 arcminutes) in both RA and DEC. Over a total observing time of about 4 hours, the VLA was cycled between these pointings, dwelling on each for about 3 minutes. The goal was to maximise the coverage of the u, v plane for each pointing. Images and beams were made using UVMAP, producing results in the AIPS SIN projection, but each with a different tangent point. For the dirty images only, reduction to a

[a] The National Radio Astronomy Observatory (NRAO) is operated by Associated Universities, Inc., under contract with the National Science Foundation.

common tangent point was accomplished using HGEOM. The resulting re-projected dirty images were pre-convolved with the same Gaussian used for the Penticton image. The input to VTESS was a collection of 22 dirty images and beams, each of size 1024^2 pixels. The primary beam for each pointing is modeled by a polynomial fit (Napier and Rots, 1982), which is truncated to zero at the 7% level. The deconvolution took 22 iterations to converge to a noise level of 1.3 mJy/beam for each field.

DISCUSSION

The final images are shown in Figure 1. For comparison, all these images have been masked on the basis of the VLA sensitivity to include only points where the noise level is less than 1.3 mJy/beam. This therefore excludes regions where only one pointing contributes to the image. The agreement between the VLA image and the Penticton image is quite good at high spatial frequencies, but poorer at lower spatial frequencies. The crucial question concerns how close to the center of the u, v plane the visibilities predicted by the VLA image are reasonably accurate. The difference image (figure 2) shows that the disagreement splits into two main parts: first, the point sources show a suprisingly amount of discrepancy. The points in the Penticton image are displaced inwards towards the image center with respect to the VLA image. The cause of this is not yet known. The second part is a discrepancy at low spatial frequencies, less than about $\frac{20m}{\lambda}$. This limit is smaller than the minimum spatial frequency measured by the VLA, of about $\frac{28m}{\lambda}$. To study this in more detail, the Penticton image was re-made with a variety of cutoffs in u, v coverage. All spacings shorter than $\frac{16m}{\lambda}$, $\frac{20m}{\lambda}$, $\frac{25m}{\lambda}$, were thrown out, and the difference between the Penticton and VLA images recomputed. The resulting difference images are shown in figure 3. The reconstructions are in good agreement for a cutoff at 20m, and in reasonable agreement at 16m, so the interpolation has been successful at interpolating inwards by between 8 and 12 meters. Figure 3(c) shows an interesting effect: the mosaiced VLA image recovers more brightness than the Penticton image with a cutoff at 25m. This is consistent with the larger dish size of the VLA which allows interpolation further in towards the center than possible with the 9m diameter dishes of Penticton.

One final point to be made is that a *joint* deconvolution is required. To demonstrate this, I re-made the VLA images in two different ways. First, I deconvolved each field separately, and then combined linearly, weighting by the primary beam as appropriate. In the deconvolution, no correction of the primary beam was made. Convergence was obtained in between 10 and 15 iterations. Secondly, I again deconvolved each field separately, but this time, I corrected each field for the primary beam in the deconvolution. One would expect this latter approach to be superior to the former, but still inferior to the joint deconvolution. This can be verified from figure 4, where both images are shown.

CONCLUSIONS

- Mosaicing works.
- For the VLA at λ20cm, it seems possible to estimate spacings about 10m shorter than the shortest actually measured. This is just less than half the dish diameter,

consistent with the truncation of the primary beam model at twice the full-width-to-half-maximum. The high declination of the source prevents much foreshortening of the VLA so that relatively few short spacings are obtained. One might therefore expect even better results for a low declination object.

- Performing the deconvolution jointly is better than separately, while both are superior to separate deconvolution with no primary beam correction. The extra computing cost in the joint deconvolution is about a factor of two for the 22 pointing centers processed here.
- The implications for MMA are quite favorable. I have shown that for a moderately complicated object and using a crude model of the primary beam, mosaicing can yield interpolation in toward the center of the u, v plane by up to half a dish diameter. Interpolation from zero outwards is also probably feasible by the same amount if the interferometer elements also measure total power. We can therefore fill the famous gap at somewhat less than a dish diameter by mosaicing alone. A single dish size will thus probably suffice. However, we need to verify this conclusion for a more realistic approximation to the MMA. In particular, pointing errors for the VLA elements at λ20cm are negligible, but may be significant for the MMA at λ0.8mm. A conclusive demonstration of this will require simulations.

ACKNOWLEDGEMENTS

I thank Rick Perley for help with the VLA observations, and John Bally and Frank Israel for providing the Penticton data.

REFERENCES

Cornwell, T.J. (1984), *NRAO mm array memo 24.*

Cornwell, T.J. (1987), *NRAO mm array memo 42.*

Napier, P.J. and Rots, A.H. (1982), *NRAO test memo 134.*

Figure 1(a) Penticton image.

PLOT FILE VERSION 8 CREATED 04-NOV-1987 09:39:06
SIMEIS 5 IPOL 1420.875 MHZ S57 PENT.CLIP.1

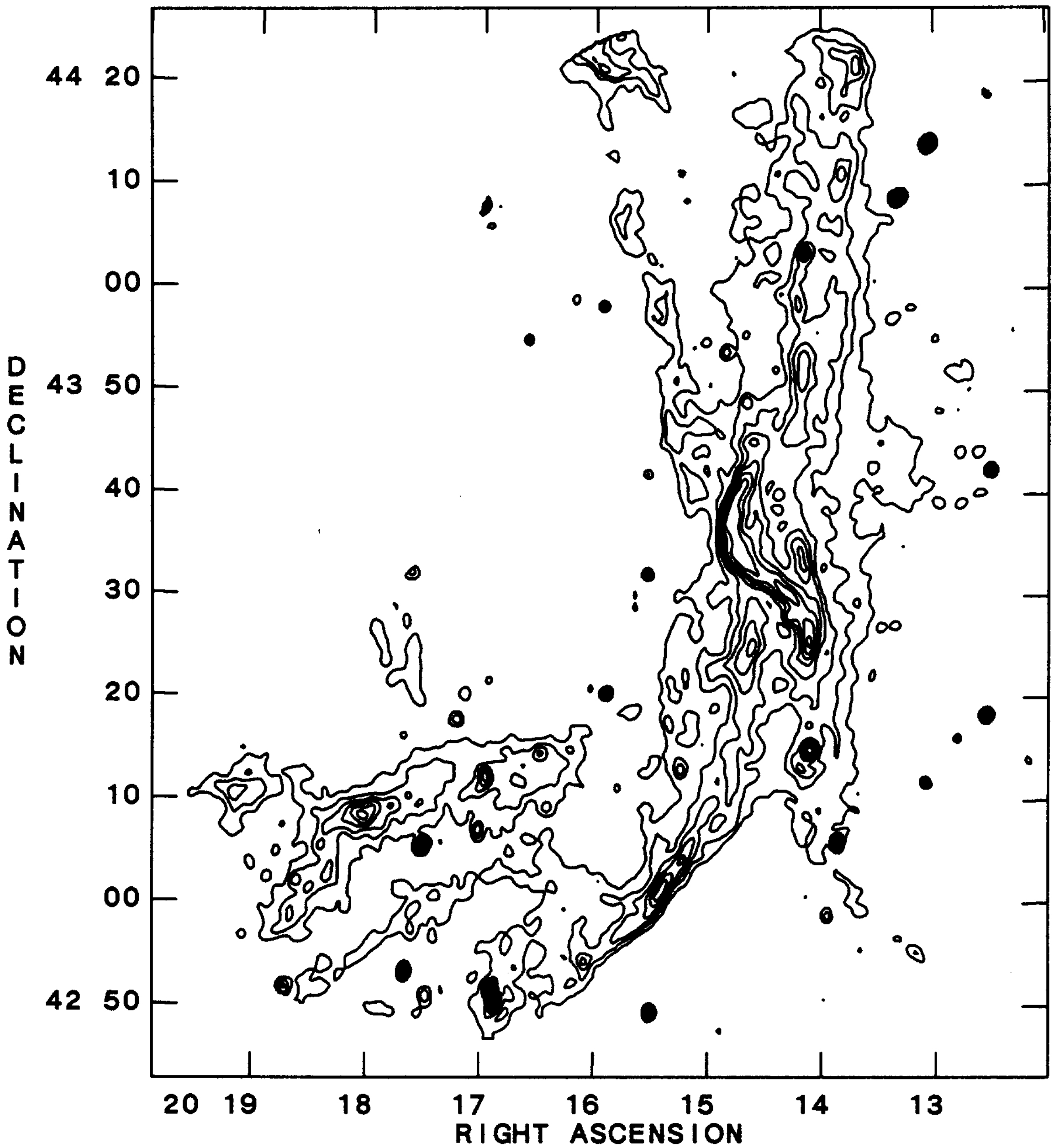

PEAK FLUX = 7.8520E-03 JY/PIXEL
LEVS = 3.0000E-04 * (-5.00, -4.00, -3.00, -2.00, -1.00, 1.000, 2.000, 3.000, 4.000, 5.000, 6.000, 7.000, 8.000, 9.000, 10.00, 11.00, 12.00, 13.00, 14.00, 15.00, 16.00, 17.00, 18.00, 19.00, 20.00)

Figure 1(b). VLA image. crosses denote pointing centers.

PLOT FILE VERSION 6 CREATED 04-NOV-1987 09:34:43

SIMEIS 5 IPOL 1395.000 MHZ S57 ALLVLA.CLIP.1

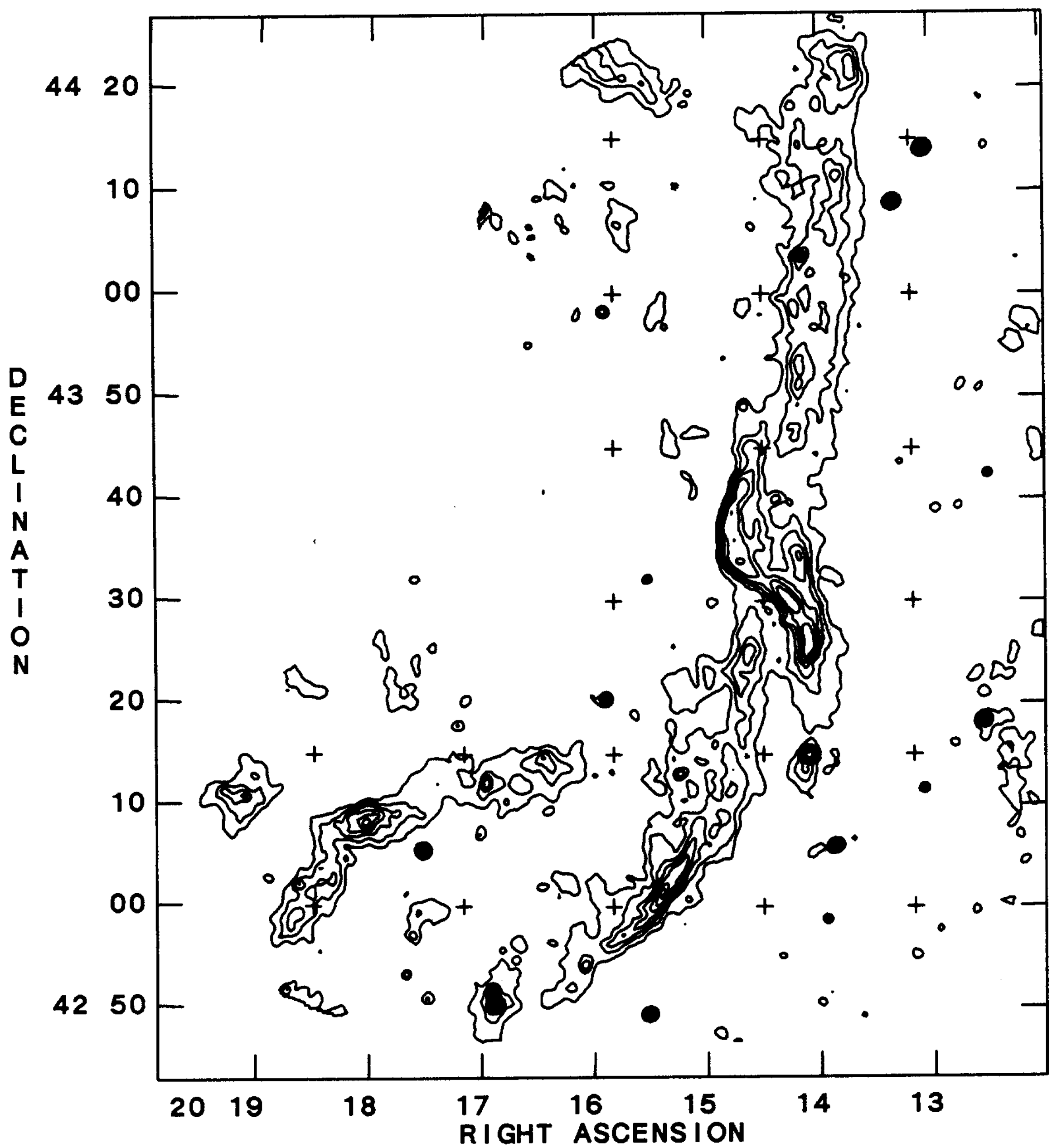

PEAK FLUX = 8.6945E-03 JY/PIXEL

LEVS = 3.0000E-04 * (-5.00, -4.00, -3.00, -2.00, -1.00, 1.000, 2.000, 3.000, 4.000, 5.000, 6.000, 7.000, 8.000, 9.000, 10.00, 11.00, 12.00, 13.00, 14.00, 15.00, 16.00, 17.00, 18.00, 19.00, 20.00)

Figure 2: Difference between Penticton and VLA images. Same contours as fig. 1.

PLOT FILE VERSION 2 CREATED 04-NOV-1987 09:43:22
SIMEIS 5 IPOL 1420.875 MHZ S57 (P-V).CLIP.1

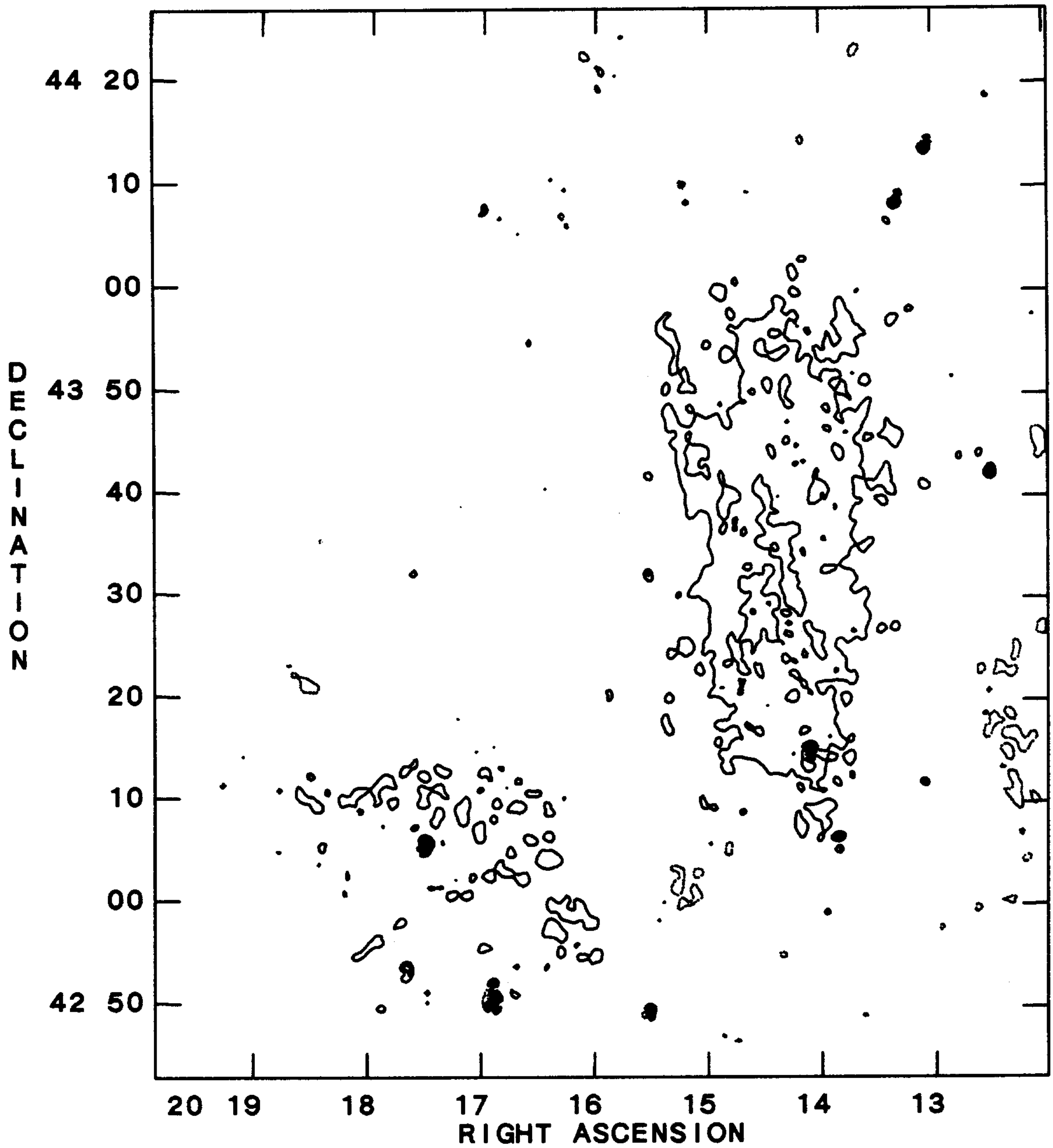

PEAK FLUX = 2.2796E-03 JY/PIXEL
LEVS = 3.0000E-04 * (-5.00, -4.00, -3.00, -2.00, -1.00, 1.000, 2.000, 3.000, 4.000, 5.000, 6.000, 7.000, 8.000, 9.000, 10.00, 11.00, 12.00, 13.00, 14.00, 15.00, 16.00, 17.00, 18.00, 19.00, 20.00)

Figure 3(a): (Penticton – VLA)

$$(u^2+v^2)^{\frac{1}{2}} > \frac{16\,m.}{\lambda}$$

PLOT FILE VERSION 1 CREATED 04-NOV-1987 11:54:48

SIMEIS 5 IPOL 1420.875 MHZ S57 (P-V).CLIP.3

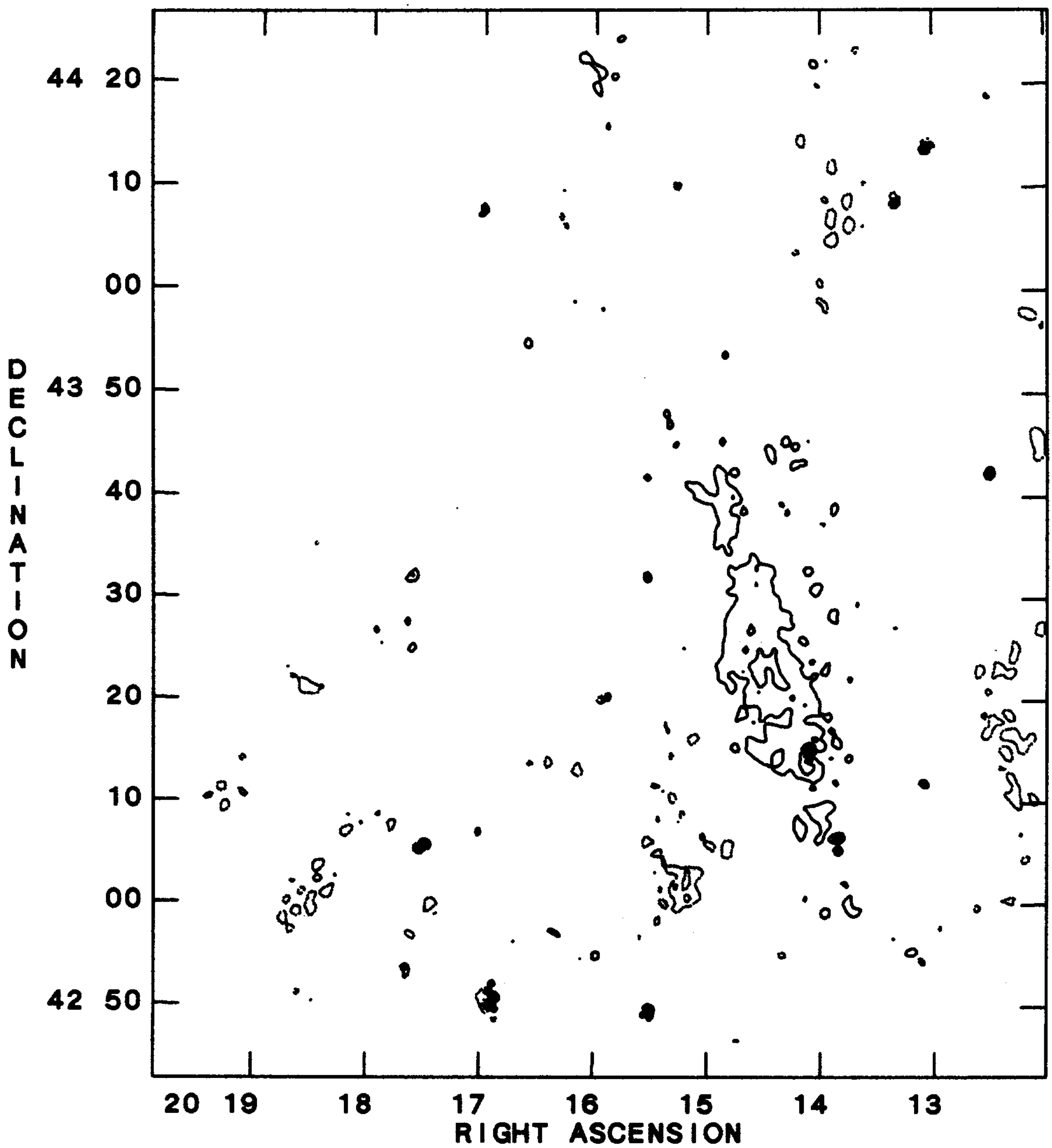

PEAK FLUX = 2.4909E-03 JY/PIXEL

LEVS = 3.0000E-04 * (-5.00, -4.00, -3.00, -2.00, -1.00, 1.000, 2.000, 3.000, 4.000, 5.000, 6.000, 7.000, 8.000, 9.000, 10.00, 11.00, 12.00, 13.00, 14.00, 15.00, 16.00, 17.00, 18.00, 19.00, 20.00)

Figure 3(b): (Penticton – VLA)

$$(u^2+v^2)^{\frac{1}{2}} > \frac{20m}{\lambda}$$

PLOT FILE VERSION 3 CREATED 04-NOV-1987 10:25:48

SIMEIS 5 IPOL 1420.875 MHZ S57 (P-V).CLIP.2

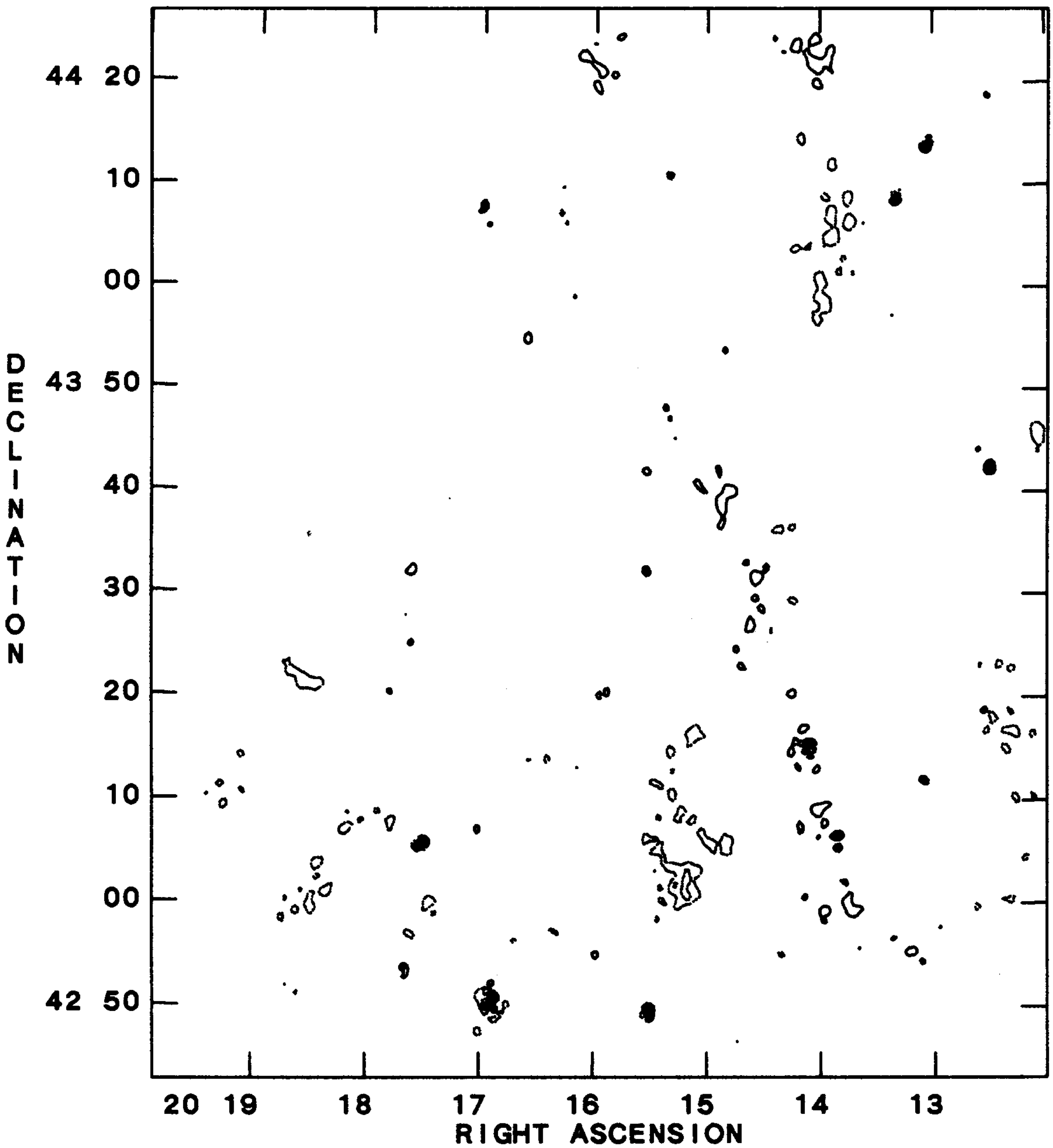

PEAK FLUX = 2.4594E-03 JY/PIXEL

LEVS = 3.0000E-04 * (-5.00, -4.00, -3.00, -2.00, -1.00, 1.000, 2.000, 3.000, 4.000, 5.000, 6.000, 7.000, 8.000, 9.000, 10.00, 11.00, 12.00, 13.00, 14.00, 15.00, 16.00, 17.00, 18.00, 19.00, 20.00)

Figure 4(a): Separate deconvolution, with no correction for the primary beam in the deconvolution.

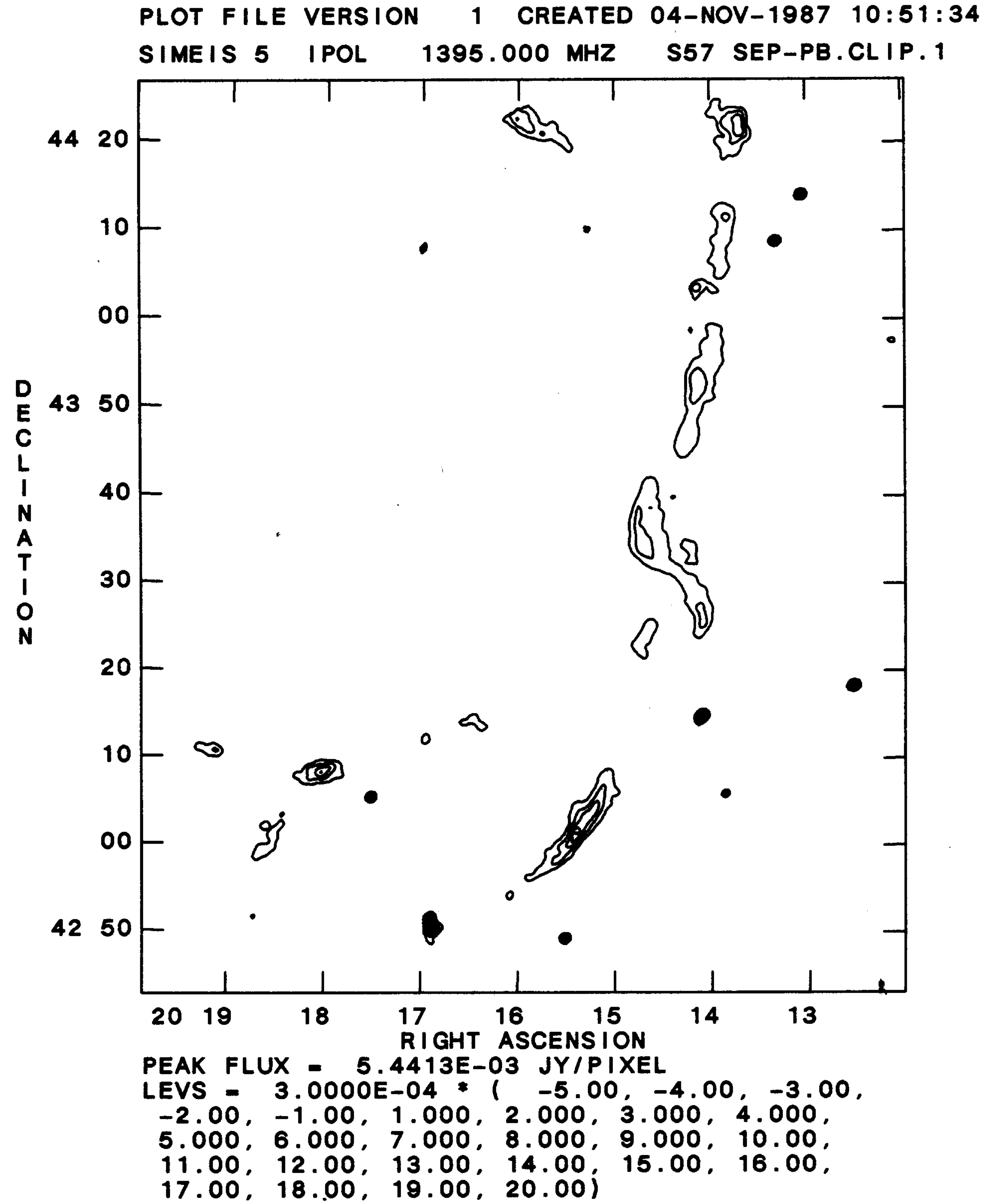

Figure 4(b): Separate deconvolution with correction for the primary beam in the deconvolution.

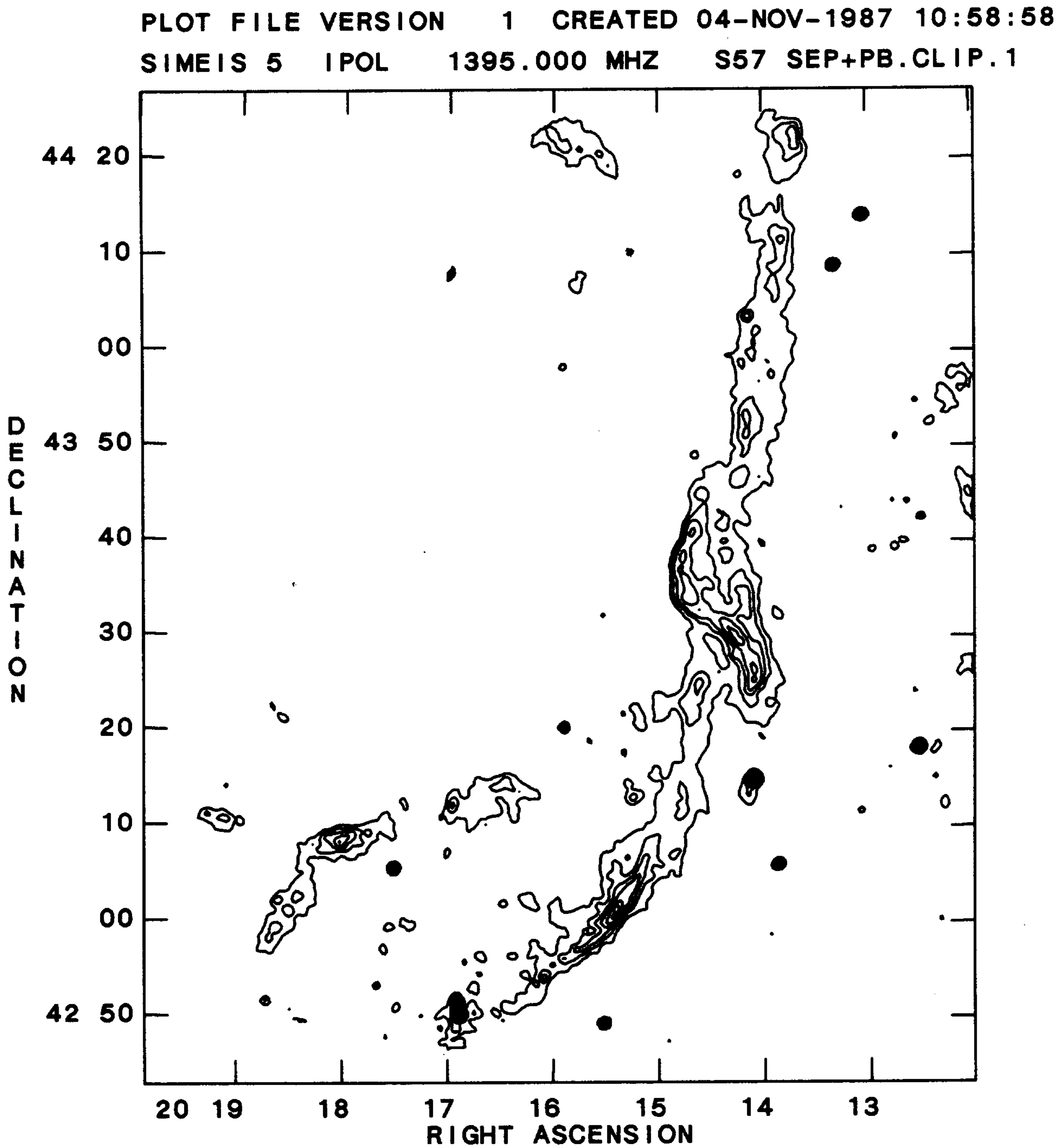

PEAK FLUX = 6.5068E-03 JY/PIXEL
LEVS = 3.0000E-04 * (-5.00, -4.00, -3.00, -2.00, -1.00, 1.000, 2.000, 3.000, 4.000, 5.000, 6.000, 7.000, 8.000, 9.000, 10.00, 11.00, 12.00, 13.00, 14.00, 15.00, 16.00, 17.00, 18.00, 19.00, 20.00)